Dual Role for Microtubules in Regulating Cortical Contractility during Cytokinesis

Kausalya Murthy and **Patricia Wadsworth**
Department of Biology and Program in Molecular and Cellular Biology University of Massachusetts at Amherst Amherst, MA 01003

Abstract

Microtubules stimulate contractile ring formation in the equatorial cortex and simultaneously suppress contractility in the polar cortex; how they accomplish these differing activities is incompletely understood. We measured the behavior of GFP-actin in mammalian cells treated with nocodazole under conditions that either completely eliminate microtubules or selectively disassemble astral microtubules. Selective disassembly of astral microtubules resulted functional contractile rings that were wider than controls and had altered dynamic activity, as measured by FRAP. Complete microtubule disassembly or selective loss of astral microtubules resulted in wave-like contractile behavior of actin in the non-equatorial cortex and mislocalization of myosin II and Rho. FRAP experiments showed that both contractility and actin polymerization contributed to the wave-like behavior of actin. Wave-like, contractile behavior in anaphase cells was Rho-dependent. We conclude that dynamic astral microtubules function to suppress Rho activation in the nonequatorial cortex, limiting the contractile activity of the polar cortex.

Keywords

Cytokinesis; actin; microtubules; myosin; Rho

Introduction

It has long been appreciated that microtubules play a key role in specifying the location of contractile ring formation in anaphase. One model for cytokinesis, equatorial stimulation, posits that microtubules deliver positive signals to the equatorial cortex, thereby locally stimulating furrow formation and ingression. The population of microtubules that are responsible for inducing furrow formation has been shown to depend on cell type: in cultured cells, interzonal microtubules of the central spindle are essential (Wheatley and Wang, 1996; Williams et al., 1995), whereas in spherical embryonic cells, astral microtubules, even in the absence of an intervening central spindle and chromosomes, play a key role (Rappaport, 1996). Recent work in *C. elegans* embryos demonstrates that, at least in these cells, both classes of microtubules contribute to furrow induction (Bringmann and Hyman, 2005; Motegi et al., 2006). Indeed, micromanipulation experiments show that bundled microtubules are the only structural component needed for furrow induction (Alsop and Zhang, 2003).

The mechanism(s) by which microtubules signal the cortex are beginning to be unraveled (Wadsworth, 2005). Direct visualization of active Rho in live cells has shown that active Rho accumulates at the equatorial cortex prior to furrow ingression and remains active at the

Correspondence: P. Wadsworth Department of Biology Morrill Science Center N. Pleasant Street Amherst, MA 01003 413-545-4877 413-545-3243 patw@bio.umass.edu .

equatorial region throughout cytokinesis (Bement et al., 2005; Yuce et al., 2005). Microtubules are required to establish and maintain the zone of active Rho (Bement et al., 2005). Microtubules contribute to local Rho activation by delivery of centralspindilin, a complex of a plus-end directed kinesin and a Rho GAP (MKLP1 and MgcRacGAP, respectively in mammalian cells) to the cortex (Mishima et al., 2002). MgcRacGAP interacts with and activates a Rho GEF (Ect2 in mammalian cells) thus generating active Rho (Kamijo et al., 2006; Nishimura and Yonemura, 2006; Yuce et al., 2005; Zhao and Fang, 2005). In support of this model, mislocalization of MgcRacGAP to the non-equatorial cortex results in ectopic furrowing (D'Avino et al., 2006) and depletion of either MgcRacGAP or Ect2 blocks cytokinesis(Kamijo et al., 2006; Nishimura and Yonemura, 2006; Yuce et al., 2005; Zhao and Fang, 2005). An important question is how Rho activation is restricted to a discrete zone at the equatorial region. One explanation is that the equatorial region receives signals from both astral centers (Bement et al., 2005). Consistent with this possibility is the recent observation that microtubules are more numerous in the equatorial region during furrow induction, at least in *C. elegans* (Motegi et al., 2006). In addition, microtubules that pass over the separating chromosomes have been shown to be differentially stable, and thus may selectively promote delivery of centralspindlin toward the equatorial region (Canman et al., 2003).

A second model for induction of cytokinesis, polar relaxation, proposes that microtubules negatively regulate tension in the polar cortex, leading to equatorial contraction (White and Borisy, 1983; Wolpert, 1960). In echinoderm eggs, the polar cortex is under less tension in anaphase and computer simulations of polar relaxation generate realistic models of cytokinesis (White and Borisy, 1983). In *C. elegans* embryos with a stabilized microtubule severing protein, katanin (Kurz et al., 2002), microtubules do not extend to the cortex, and ectopic furrows develop. Similarly in cultured cells lacking microtubules, the cortex of anaphase cells shows contractile activity during a period that has been termed C-phase (Canman et al., 2000). These experiments show that the entire cortex is capable of ingression and that microtubules suppress cortical contractility. Further support for a role of the polar cortex in cytokinesis comes from experiments in which localized application of cytochalasin to the polar, but not equatorial cortex, blocks cytokinesis (O'Connell et al., 2001).

Taken together these data suggest that microtubules both positively induce contractile ring assembly by local activation of Rho and negatively regulate contractile ring formation by inhibiting the formation of ectopic furrows. In support of this recent work in *C. elegans* shows that astral microtubules regulate the recruitment of cortical myosin (Werner et al., 2007). How microtubules can simultaneously function as both positive inducers and negative regulators of cytokinesis is puzzling.

In the experiments reported here, contractile ring assembly in mammalian epithelial cells expressing GFP-actin (Murthy and Wadsworth, 2005) has been examined following treatment with nocodazole to differentially disassemble microtubules in anaphase cells. Complete elimination of microtubules, by addition of nocodazole within 2 minutes of anaphase onset, blocks cytokinesis. In contrast when only non-equatorial astral microtubules are eliminated by addition of nocodazole > 2 minutes after anaphase onset, cytokinesis proceeds to completion, demonstrating that under these conditions astral microtubules are dispensable for furrow ingression. We show that cells lacking astral microtubules display wave-like, contractile activity of cortical actin that requires Rho, and its downstream targets, and further show that Rho and myosin RLC are mislocalized to the polar cortex of these cells. Our data demonstrate that dynamic astral microtubules negatively regulate actomyosin in the polar cortex by preventing Rho activation and, simultaneously, stable interzonal microtubules activate Rho in the equatorial region.

Materials and Methods

Materials

All materials for cell culture were obtained from Sigma-Aldrich, St. Louis, MO, with the exceptions of Opti-MEM, Trypsin and Lipofectamine2000 which were obtained from Invitrogen, Carlsbad, CA and fetal bovine serum, which was obtained from Atlanta Biologicals, Norcross, GA. C3 transferase and cell permeable C3 transferase were obtained from Cytoskeleton, Inc, Denver CO. All other chemicals were obtained from Sigma-Aldrich unless otherwise noted.

Cell culture and inhibitors

Cell culture was performed as previously described (Murthy and Wadsworth, 2005). Before use in experiments, cells were plated on clean coverslips and imaged within 48 hours. GFP-tubulin and GFP-actin expressing LLC-Pk1 cells have been described previously (Murthy and Wadsworth, 2005; Rusan et al., 2001). LLC-Pk1 cells expressing TDRFP-myosin regulatory light chain were prepared as described previously using human myosin regulatory light chain fused to TDRFP (gift of Dr. G. Charras). Live imaging of RhoA localization was performed by transiently transfecting LLC-Pk1 cells with a *C.elegans* Rho probe (Yuce et al., 2005) (gift of Dr. M. Glotzer) using Lipofectamine2000. We used GFP-tagged *C. elegans* RhoA, rather than the YFP-tagged *C. elegans* RhoA for compatiblity with our microscope filters. Only cells with a moderate level of expression of the GFP-tagged *C. elegans* Rho A were utilized in experiments. To inhibit Rho, cells were either microinjected with C3 transferase (pipette concentration 0.5 –1.0 mg/ml), or cells were incubated with 2.5 μg/ml cell permeable C3 transferase (both from Cytoskeleton Inc., Denver, CO) for at least 4 hours prior to imaging. The efficacy of the cell permeable C3 transferase was evaluated by the disruption, or reduction, of stress fibers in neighboring cells, and changes in cortical behavior. Nocodazole was used at 33 μM, both Y27632 and ML-7 were used at 50 μM, and (-)-blebbistatin (EMD BioSciences, San Diego, CA) was used at 75 μM.

Immunofluorescence microscopy

To stain for RhoA, cells were fixed 15 min in 10% ice cold TCA (v/v), then rinsed in PBS containing 30 mM glycine (PBS-G). Cells were lysed in 0.2% Triton-X-100 (v/v) in PBS-G for 5 min, and incubated with anti-RhoA antibodies diluted 1:100 (Santa Cruz Biotechnology, Inc. Santa Cruz, CA) in PBS-Tw-Az (PBS containing 0.1% Tween-20 and 0.02% sodium azide) supplemented with 1 mg/ml BSA for 1 hr at 37° C. To stain for phosphorylated myosin, cells were fixed in 3.7% formaldehyde (v/v) or 0.25% glutaraldehyde (v/v) rinsed in PBS-Tw-Az and incubated with phospho-myosin light chain 2 (Thr18/Ser19) antibodies (Cell Signaling Technology, Beverly, MA) at a 1:100 dilution. Fluorescein and Cy3 conjugated secondary antibodies were obtained from MP Biomedicals (Solon, OH) and Jackson Immuno Research Laboratories, Inc. (West Grove, PA) respectively and used according to the manufacturers specifications. Actin was stained with Alexa 488 phalloidin by incubation for 10 minutes (Invitrogen Corp., Carlsbad, CA).

Image acquisition and analysis

Images were obtained using a Perkin Elmer (Perkin Elmer, Freemont, CA) spinning-disc confocal scan head attached to a Nikon TE300 microscope (Nikon, Inc.) as described previously(Rusan et al., 2002). The microscope and peripherals were driven by Metamorph software (Molecular Devices, Sunnyvale, CA). Typically, images (500-800 msec exposures) were obtained at 10-20 second intervals for the duration of cytokinesis. For immunofluorescence images, maximum intensity projections of Z-stacks (0.2 μm step size) were generated in Metamorph. Photobleaching experiments were performed using a Zeiss 510

Meta scanning confocal system(Murthy and Wadsworth, 2005). For photobleaching in untreated cells, an initial image was acquired while the cell was in anaphase, and then photobleaching was performed (Murthy and Wadsworth, 2005) and images were acquired every 5 sec for 2-3 min. For photobleaching experiments in nocodazole treated cells, an initial image was acquired when a cell was in anaphase, prior to drug application, and then another image was acquired following nocodazole addition. The cell was photobleached as for control cells and then images were acquired every 5 sec for 2-3 min. Turnover ($t_{1/2}$) of the bleached region was calculated as the time required to attain half of the final intensity. As a control, the intensity in an unbleached region was monitored.

The width of the contractile ring was measured and expressed as a percentage of cell length as follows. First, we measured the width of the band of F-actin organized perpendicular to the spindle axis. Then the cell length was measured, also along the spindle axis. Measurements were made just prior to ingression for both control and nocodazole treated cells. The percentage of cell length occupied by contractile ring was then calculated.

In both untreated as well as nocodazole treated cells, actin accumulation was determined by measuring the change in fluorescence intensity of GFP-actin in a selected area of the equatorial cortex as the cell progressed from anaphase onset into telophase. The percent increase from the initial fluorescence value was determined and the average of the maximum increase for each cell was calculated.

The average fluorescence intensity of actin in the contractile ring was determined by measuring the fluorescence intensity in a 2.6 μm by 2.8 μm box for control (n = 7) and late nocodazole cells (n = 9) and averaging the values. For this measurement, raw values from images that were not scaled were used.

Results

Differential stability of microtubules in anaphase cells

To examine the role of microtubules in regulating contractile ring formation and ingression, we treated LLC-Pk1 cells expressing GFP-tubulin with a high concentration of nocodazole to induce rapid disassembly of microtubules. When 33 μM nocodazole was added within 2 minutes of anaphase onset, microtubules completely disassembled, as determined by imaging GFP-tubulin (Figure 1A, n = 6). Microtubule disassembly was complete within a few minutes of drug application, and both cortical ingression and cytokinesis were prevented under these conditions. We will refer to these cells as "early-nocodozole" cells. In contrast, when cells were treated with 33 μM nocodazole more than 2 minutes after anaphase onset (hereafter, "late-nocodozole" cells), astral microtubules disassembled, but interzonal microtubules were differentially stable (Figure 1B, n = 5). In these cells, cortical ingression and cytokinesis occurred, resulting in the formation of two daughter cells, although complete abscission, which requires several hours to complete, was not monitored. These results demonstrate that interzonal microtubules acquire differential stability to nocodazole by two minutes after anaphase onset and that astral microtubules are dispensable for furrow ingression. Consistently, interzonal microtubules have been shown to be necessary for cytokinesis in a variety of cell types (Raich et al., 1998; Wheatley and Wang, 1996; Williams et al., 1995). The differential stability of astral and interzonal microtubules allowed us to isolate the contribution of astral microtubules to contractile ring formation and function.

Observations on the contractile ring formed without astral microtubules

To examine actin organization during contractile ring formation and ingression, we imaged LLC-Pk1 epithelial cells expressing GFP-actin using spinning-disc confocal microscopy

(Murthy and Wadsworth, 2005). Except when noted, actin in the ventral cortex was imaged, because in adherent cells, actin in the dorsal cortex is less well organized (Fishkind et al., 1996). As described previously, actin was uniformly distributed in the cortex prior to anaphase and then actin filaments accumulated at the equatorial region (Figure 2A; Movie 1). Actin accumulation in the ring was determined by measuring the increase in the GFP-actin fluorescence intensity. As control cells (n =6) progressed from early to late anaphase, GFP-actin fluorescence within the equatorial region increased by $33 \pm 16.1\%$. Within the contractile ring, actin filaments were arranged in discrete bundles perpendicular to the spindle pole-to-pole axis, while at the periphery of the ring, actin filaments were arranged at various angles (Figure 2A) (Mandato and Bement, 2001). In some cells, following the initial accumulation of actin at the equator, actin adjacent to the equatorial region was observed to flow towards the contractile ring (Cao and Wang, 1990; Zhou and Wang, 2008).

In early-nocodozole cells, consistent with the lack of visible furrowing, the extent of GFP-actin accumulation at the equatorial region was greatly reduced if not eliminated (Figure 2B). Thus, the failure of these cells to initiate and undergo cytokinesis reflects the failure to form, rather than to activate, a contractile ring. In late-nocodazole cells, GFP-actin accumulated at the equatorial region and furrow formation and ingression were completed in nearly all cells examined (15/16) (Figure 2C, D).

Given that furrow formation and ingression succeed in late-nocodazole cells, we verified that two components of functional contractile rings accumulated at the furrow in these cells: namely, membrane-associated, and thus active, Rho (Nishimura and Yonemura, 2006) and phosphorylated, and thus active, myosin II. We localized Rho in cells expressing GFP-RhoA from *C. elegans* (hereafter GFP-CeRhoA). Previous work showed that fluorescently tagged CeRhoA localized to the equatorial cortex in a distribution that was similar to the distribution of RhoA determined by immunofluorescence microscopy of TCA fixed cells stained with RhoA antibodies (Nishimura and Yonemura, 2006; Yuce et al., 2005). In control LLCPk1 cells, GFP-CeRhoA fluorescence accumulated at the equatorial cortex just prior to ingression, and remained at the site of ingression throughout cytokinesis (Figure 3A). GFP-CeRhoA also localized to the centrosomal region, at membranous folds at the cell periphery, and at cell membranes where adjacent cells were in contact (Figure 3A; Movie 2). This distribution was observed in both live cells expressing GFP-CeRhoA and in TCA fixed and stained cells (see Suppl. Fig. 4). In early-nocodazole cells, GFP-CeRhoA did not detectably accumulate at the equatorial cortex (Figure 3B), consistent with results above showing these cells do not form a contractile ring; whereas, in late-nocodazole cells, GFP-CeRhoA localized to the equatorial region at the site of cortical ingression (Figure 3C). Likewise, in control and late-nocodazole cells, myosin II was present throughout the cortex at metaphase and became restricted following anaphase to the equatorial cortex (data not shown). In addition, phosphorylated myosin regulatory light chain, which is required for activation of myosin and filament formation, was present at the equatorial region of control and late nocodazole cells. This demonstrates that myosin II at the equatorial cortex is active (Supplemental Figure 1). These results indicate that the functional contractile rings forming in late-nocodazole cells resemble controls insofar as they contain membrane-associated Rho and active myosin II.

In the late-nocodozole cells, although the contractile ring formed, it appeared wider than in control cells and was associated with an increase in the number and length of bundles of GFP-actin oriented perpendicular to the ring (Figure 2 C, Movie 3). The width of the contractile ring, measured as a percent of cell length (see Methods), increased significantly, from 16% in control cells to 26% in the late nocodozole cells (n = 11). The increase in the width of the contractile ring could reflect the same quantity of actin filaments dispersed over a larger area of the cortex or a net increase in filamentous actin, for example as a result of flow. To distinguish between these possibilities, we measured GFP-actin fluorescence intensity within the ring. The

average fluorescence intensity was not statistically significantly different between control and treated cells (1159 ± 252 versus 1277 ± 282 respectively), yet the area occupied by the ring was greater, demonstrating that more actin is present in the equatorial region of cells lacking astral microtubules. Furthermore, actin in the contractile ring formed in late-nocodozole cells had altered dynamics, indicated by a statistically significant two-fold reduction in the half-time for recovery of fluorescence following photobleaching and a reduction in the extent of recovery (Table 1). Taken together, although a functional contractile ring forms in the absence of astral microtubules, it differs from one made in the presence of those microtubules in being broader and more dynamic.

Cortical actin behavior in the complete absence of microtubules

Surprisingly, in nocodozole-treated cells, GFP-actin fluorescence in the cortex increased and decreased in a wave-like manner. In early-nocodozole cells, the wave-like changes in GFP-actin fluorescence occurred throughout the cortex and moved both toward and away from the equatorial region (Figure 2B, inset). Although difficult to discern in still images, this dynamic behavior of actin is unmistakable in time-lapse sequences (Movie 4). In some cells, waves appeared to initiate repeatedly at a single region of the cortex, whereas in others, they appeared to initiate at multiple sites. The rate of apparent motion of actin, estimated by tracking regions of increased GFP-actin fluorescence, was 50 ± 9 μm/min. Wave-like behavior of actin was never observed in control cells and is distinct from cortical ruffles, which were observed on the dorsal cortex of both control and nocodazole-treated cells. In late-nocodozole cells, wave-like behavior of cortical actin was often seen outside of the equator, but in these cells there was also a directed flow of cortical actin toward the equator. Most late-nocodozole cells showed both behaviors, with the fraction of cortical actin that participated in each behavior varying from cell to cell (Figure 2, C and D; Movie 3). Although wave-like behavior was random with regard to direction, flow was directed toward the equator, where the material contributed to contractile ring formation (Figure 2D). Apparently, the absence of astral microtubules sets up conditions permissive for an unusual state of actin organization.

Because actin fluorescence propagating across the cortex in waveforms is unusual, we investigated this phenomenon further. Waveforms could result from bulk movement of unpolymerized actin, from actin filament polymerization and depolymerization, or from sequential contraction and relaxation of cortical regions that would change the density and thus fluorescence of actin. To test these possibilities, we used photobleaching to place marks on GFP-actin. If cortical contraction contributes to wave-like behavior, then the bleached region should become distorted; if polymerization and depolymerization contribute, then the bleached region should remain stationary (Theriot et al., 1992). Following photobleaching, the bleached region could be detected for ~ 1 minute, indicating that fluorescence was due, at least in part, to assembled F-actin; diffusive motion of unpolymerized G-actin occurs much more rapidly. In most cells, the photobleached mark was distorted, indicating that cortical contractions contributed to actin dynamics (Figure 4; Movie 5). However, the bleached region also filled in with GFP-fluorescence, indicating actin polymerization. Recovery of fluorescence without detectable motion is consistent with the observations that the entire cortex is not simultaneously contractile. It appears that both cortical contraction/relaxation as well as actin polymerization/depolymerization contribute to the observed oscillation of actin fluorescence.

We tested the possibility that microtubules regulate cortical actomyosin interactions throughout mitosis, not only in anaphase. To do this, we treated GFP-actin cells with (33 μM) nocodazole, which disassembles microtubules completely at all phases of mitosis (except as noted above for interzonal microtubules in late anaphase), and imaged cells containing condensed chromosomes within 20 minutes of treatment. Nearly all mitotic cells showed contractile wave-like behavior of cortical actin that was similar to that observed in anaphase

cells, although often more robust (Supplemental Figure 2A). Because mitotic cells are more numerous than anaphase cells and multiple experimental cells can be imaged per coverslip, FRAP experiments were also performed on mitotic cells. Consistent with results in anaphase cells, both contractile activity and polymerization contributed to recovery of the photobleached mark (Supplemental Figure 2 B, Movie 6). Note that wave-like behavior of actin was never seen in control mitotic cells containing microtubules.

Given that the FRAP experiments demonstrated contractile behavior of the cortex in nocodazole-treated cells, we examined the distribution and dynamics of myosin in the non-equatorial cortex. To do this, we prepared an LLC-Pk1 cell line expressing MRLC fused to a tandem dimer of red fluorescent protein (hereafter TDRFP-MRLC) (Charras et al., 2006). RFP-MRLC appeared as puncta in the cell cortex. In control and late-nocodozole cells, the puncta accumulated during late anaphase in a distinct band at the equatorial region (Figure 5A, C; Movie 7). During ring formation and ingression, RFP-MRLC puncta, aligned in a linear fashion, flowed from cortical regions adjacent to the equator toward the forming ring. These results are consistent with previous observations of myosin II and its regulatory kinase (Cao and Wang, 1990; DeBasio et al., 1996), but differ from observations of non-muscle myosin IIA heavy chain (Zhou and Wang, 2008). In early-nocodazole cells, RFP-MRLC failed to localize at the equator and remained dispersed throughout the cortex (Figure 5B); in some cases, puncta of RFP-MRLC were observed to coalesce and disperse in regions of the cortex, but were not translocated across the cell. In late-nocodazole cells, myosin puncta accumulated at the equatorial cortex as in control cells and were mislocalized to the non-equatorial cortex in three out of six cells (Movie 8). Myosin in the non-equatorial cortex was dynamic, undergoing dispersion and coalescence, but wave-like propagation across the cell was not observed (Figure 5C, arrows, Movie 8). Thus, the dynamic behavior of actin and myosin RLC in the cortex of late nocodazole cells was distinct.

Assaying activators of cortical actin behavior

Next, we tested the possibility that the nocodazole-induced changes in cortical actomyosin in anaphase cells require the activity of the small GTPase RhoA. First, we examined the distribution of GFP-CeRhoA in the non-equatorial cortex of late-nocodazole cells. In these cells, GFP-CeRhoA fluorescence fluctuated in a wave-like manner similar to what we observed for GFP-actin (Figure 6A, Movie 9). Previous workers have shown that the level of cortical fluorescence of the CeRhoA probe reflects the level of Rho activation: overexpression of the GAP domain from mouse RhoGAP1, which reduces active Rho, reduced cortical fluorescence and conversely, overexpression of the GEF domains from the Rho GEF, ECT2, which increases GTP bound, active Rho, increased cortical fluorescence (Yuce et al., 2005). Thus, one interpretation of the dynamic pattern of GFP-CeRhoA fluorescence in the polar region of nocodazole treated cells is that the loss of microtubules induces activation of Rho in the polar region and that once activated, Rho undergoes dynamic cycles of activation and inactivation. In these images, we focus on the cell cortex, but using the light microscope we cannot determine if the fluorescence is exclusively from membrane associated, and thus active GFP-CeRhoA, or if it includes cortical, but not membrane associated fluorescence. To learn if the Rho is membrane associated, we reexamined the distribution of RhoA in the non-equatorial cortex of nocodazole treated cells fixed with TCA, a method that preserves membrane associated, but not cytoplasmic RhoA (Nishimura and Yonemura, 2006). In these cells, RhoA was mislocalized to non-equatorial sites, consistent with the hypothesis that the GFP-CeRhoA is active (Supplemental Figure 4).

To determine whether Rho activity was required for the wave-like behavior of actin, we used C3 transferase, which ADP-ribosylates, and thus inactivates, Rho (Sekine et al., 1989). Previous work has shown that adherent cells can complete cytokinesis following inhibition of

Rho with C3 transferase (O'Connell et al., 1999). Three out of seven LLC-Pk1 cells expressing GFP-actin that were injected in metaphase with C3 transferase completed furrow formation and ingression, as did seven out of ten cells that were injected in anaphase and five out of six cells treated with a cell-permeable C3 transferase (data not shown). Furrows that formed in C3 treated cells were wider than normal and these cells showed cortical blebbing (data not shown). To test the contribution of Rho to the wave-like behavior of cortical actin, cells were treated with cell-permeable C3 transferase, observed until the onset of anaphase, and nocodazole was added. This treatment blocked wave-like behavior in five out of six cells, although some limited, local contractions were observed. In a second test of the role of Rho in cortical wave-like activity, cells expressing GFP-actin were followed into anaphase, nocodazole was added to induce cortical wave-like behavior and the cells were microinjected with C3. Similarly, within several minutes of C3 transferase injection, actin waveforms diminished (Figure 6B, B'). These results indicate that active Rho is required for wave-like behavior of actin in the cell cortex, at least during anaphase. In mitotic cells that were treated with nocodazole, however, C3 was less effective in blocking the wave-like behavior, suggesting that myosin activity is regulated in a cell cycle dependent manner.

To identify the downstream effectors of Rho that mediate the changes in cortical actin behavior, an inhibitor of Rho kinase, Y27632 (Uehata and Narumiya, 1997) was added to nocodazole-treated anaphase cells. Actin wave-like behavior was inhibited within one minute following addition of Y27632 (n = 4), demonstrating that phosphorylation by Rho kinase contributes to actin wave-like behavior (Figure 6C and C'). As one of the known targets of Rho kinase is myosin II, we also examined wavelike behavior following addition of ML-7, an inhibitor of myosin II light chain kinase, to nocodazole treated cells. ML-7, like Y27632, suppressed wave-like behavior of actin within several minutes (data not shown). This result suggests that myosin II activity contributes to wave-like cortical actin behavior in these cells, although ML-7 may target other kinases in the cell. We also treated cells with blebbistatin (Straight et al., 2003) to inhibit myosin and then added nocodazole after anaphase onset. Because blebistatin is inactivated at the wavelength used to image GFP (Kolega, 2004), we cannot image the wave-like behavior of GFP-actin directly in this experiment. Rather, we monitored TD-RFP-MRLC in the polar cortex. In blebistatin treated cells that were in early anaphase at the time of nocodazole addition, some cortical myosin accumulated at the equatorial region of the cell, but much remained dispersed throughout the cortex and dispersion and coalescence of puncta of TD-RFP-MRLC in the polar cortex was not detected (Supplemental Fig. 3). This result indicates myosin activity contributes to contractile activity in the polar cortex.

Although the wave-like behavior of cortical actin was sensitive to inhibition of Rho and its downstream targets, flow of cortical actin toward the equatorial region was not. Treatment of late nocodazole cells with C3 or Y27632 did not inhibit directed motion of actin toward the equator, and robust contractile rings formed in these cells. These observations suggest that equatorial flow of actin is distinct from the formation of waveforms throughout the cortex.

Discussion

Together, these results show that the complete disassembly of microtubules in anaphase results in the inability to accumulate actin to form a contractile ring and, in addition, induces a wave-like behavior of cortical actin and mislocalization of myosin RLC and active RhoA. In contrast, cells that lack astral microtubules but retain interzonal microtubules show both wave-like behavior and the formation and function of the contractile ring, although with slightly altered properties. These results highlight the importance of the astral microtubules in regulating the behavior of the cell cortex throughout anaphase.

We found that microtubules are completely disassembled when nocodazole is added within two minutes of anaphase onset but when the same concentration of nocodazole is applied >2 min after anaphase onset interzonal microtubules are no longer sensitive to nocodazole and cytokinesis is completed. Thus, at least 2 min is needed for microtubules to alter the cortex so that cytokinesis proceeds; simultaneously interzonal microtubules become resistant to nocodazole. The interzonal microtubules that are retained in late-nocodazole treated cells are sufficient to maintain the equatorial zone of active Rho and active myosin in the absence of astral microtubules.

Wave-like behavior of actin has been observed in motile interphase *Dictyostelium* cells and in cells recovering from actin disassembly (Gerisch et al., 2004). Flow of cortical actin in interphase cells is thought to result from local relaxation of the actomyosin cortex (Paluch et al., 2006). Wave-like flows of interconnected foci of cortical myosin, that move relative to one another and toward the anterior pole, have been observed following fertilization and establishment of polarity in *C. elegans* embryos (Munro et al., 2004); this behavior requires actomyosin and is Rho dependent. In anaphase cells, ectopic furrows have been observed in cells that lack, or have reduced microtubule arrays (Canman et al., 2000; Kurz et al., 2002) but the wave-like behavior of actin was not observed in these cells. In the mammalian cells examined here, we detected wave-like behavior of cortical actin and of GFP-CeRhoA. The wave-like behavior of active GFP-RhoA is novel; however we have been unable to generate a permanent cell line expressing GFP-RhoA to further examine the mislocalized Rho. Finally, we observed that polymerization and contractile activity of actin are coordinated; we did not detect halos of reduced GFP-actin fluorescence adjacent to regions that showed contractile activity as has been observed during wound healing in *Xenopus laevis* oocytes (Mandato and Bement, 2001).

We demonstrate that astral microtubules prevent activation of the small GTPase Rho, and that microtubule disassembly induced Rho-dependent actomyosin wave-like, contractile behavior and transient accumulation of membrane associated Rho in the non-equatorial cortex. In contrast, others have shown that microtubules function to generate a well-defined equatorial zone of active Rho that precedes furrow formation (Bement et al., 2005). This zone of active Rho is established, at least in part, by MKLP1 mediated delivery of MgcRacGAP to the equatorial region, where it binds and activates the Rho GEF, ECT2 (Jantsch-Plunger et al., 2000; Mishima et al., 2002; Nishimura and Yonemura, 2006; Yuce et al., 2005). Following initial Rho activation, Rho itself may contribute to microtubule stability (Palazzo et al., 2001) thus generating a positive feedback loop to ensure the continued delivery of Rho regulators to the equatorial region and completion of cytokinesis (Wadsworth, 2005).

How might microtubules simultaneously stimulate contractile activity at the equatorial region and suppress contractility in the polar cortex? We propose that the dynamic turnover of astral microtubules prevents effective delivery of regulators of Rho to the cortex and prevents the level of active Rho from reaching a critical threshold needed for contractile activity (Figure 7). This hypothesis is supported by our results and previous work which demonstrate that astral microtubules are more dynamic than interzonal microtubules in a variety of cell types (Canman et al., 2000;Kurz et al., 2002). Regulation of cortical contractility by Rho is consistent with the requirement for the Rho GEF, Ect-2, during polarity establishment in *C. elegans* (Motegi and Sugimoto, 2006) and the observation that mislocalization of RhoGAP to the non-equatorial cortex of *Drosophila* cells induces ectopic furrows (D'Avino et al., 2006). Centralspindilin, which regulates Rho at the equatorial region, can bind astral microtubules as well as interzonal microtubules, and thus could regulate Rho in the polar region as well (Nishimura and Yonemura, 2006). Depletion of the Rho GEF Ect2 results in mislocalization of active Rho throughout the cortex demonstrating that Ect2 restricts the location of Rho activity in anaphase. This observation is consistent with the proposal that microtubules contribute to the spatial

restriction of Rho activation (Birkenfeld et al., 2007). Finally, in interphase cells microtubule disassembly leads to Rho activation by release of microtubule bound GEF-H1, supporting the idea that release of Rho activators from microtubules leads to Rho activation (Krendel et al., 2002). In mitotic cells this GEF-H1 has been recently shown to contribute to spindle assembly and to the late events of cytokinesis, but its contribution to cortical contractility is not known (Bakal et al., 2005;Birkenfeld et al., 2007).

Although our data are consistent with the hypothesis that dynamic astral microtubules in the polar region fail to effectively deliver activators of Rho in a coordinated manner, an additional possibility is that different populations of microtubules may bind and deliver distinct regulators of cytokinesis (Motegi et al., 2006). For example, in *C. elegans*, microtubules that form in a gamma-tubulin dependent manner in early anaphase stimulate furrowing whereas microtubules that form in an Aurora-A kinase dependent manner later in anaphase suppress furrowing. Regardless of the exact manner in which astral microtubules function, complete microtubule disassembly, or changes in microtubule dynamics, would release or mislocalize regulators of Rho resulting in global, rather than restricted, Rho activation. Rho may contribute to cortical contractility not only by activation of myosin II, but also by stimulating actin assembly, either directly, by Rho dependent activation of formins (Watanabe et al., 1997), or indirectly, via the activation of myosin II-based contractions (Benink et al., 2000).

Our data show that dynamic astral microtubules modulate, but do not eliminate Rho activity. Cells lacking astral microtubules maintain cortical integrity, in contrast to cells in which Rho is inhibited which do not (O'Connell et al., 1999). The extent of Rho activation in the polar cortex upon microtubule disassembly is less than observed at the equatorial cortex, based on the relative fluorescence intensities of GFP-CeRhoA in the polar and equatorial regions and the fact that, in most cells, only transient contractions and wave-like activity were observed. In addition, the data show that the entire cortex can respond to an elevation in the level of active Rho. This is consistent with the results of classic experiments showing that when the spindle is displaced, the region of the cortex that the spindle comes to lie near can generate a furrow (Rappaport, 1996) and with recent results showing that non-equatorial regions of the cortex can respond to local perturbations with a contractile response (Effler et al., 2006).

Our data also show that astral microtubules limit the accumulation of actin at the equatorial region during cytokinesis. As compared with control cells, the amount of actin in the equatorial cortex was increased in cells that lack astral microtubules, but retain interzonal microtubules. This could result from increased assembly and/or decreased disassembly of actin in the equatorial region or from increased recruitment of actin from the polar regions (Cao and Wang, 1990; Guha et al., 2005). Our observations of flow of actin toward the ring, and previous observations linking microtubules to regulation of cortical flow (Benink et al., 2000) support the second possibility. Microtubules might physically restrict cortical flow either indirectly or directly via interactions with actin (Benink et al., 2000). Broad zones of active Rho have also been noted following treatment with nocodazole or depletion of MKLP1, although in these cases cells were treated prior to anaphase onset, so the broad zones may reflect a reduction or spreading of the equatorial signal(Bement et al., 2005; Yuce et al., 2005). Although cytokinesis was not markedly perturbed in late nocodazole cells that assemble larger than usual contractile rings, the duration of cytokinesis in LLC-Pk1 cells is variable, so we cannot rule out the possibility that changes in the duration of cytokinesis occurred.

Finally, our observation that inhibition of Rho with C3 did not prevent cytokinesis in the majority of C3 injected cells (O'Connell et al., 1999; Yoshizaki et al., 2004) supports the view that secondary, Rho-independent pathways contribute to cytokinesis in these adherent cells (Kanada et al., 2005). Additional Rho family members, such as Rac and Cdc42 (Yoshizaki et al., 2003), phosphoinositide signaling, and products of phosphoinositide metabolism such as

Ca^{++} ions, may also regulate various aspects of cytokinesis (Janetopoulos and Devreotes, 2006). Recent work implicates LET-99, a DEP domain protein, and heterotrimeric G proteins in aster positioned cytokinesis (Bringmann et al., 2007). Together these observations strongly suggest that, at least in these adherent mammalian cells, more than one pathway contributes to cytokinesis. Given that successful cytokinesis is so important for cell viability, the possibility of redundant pathways should not be surprising (Guha et al., 2005).

Supplementary Material

Refer to Web version on PubMed Central for supplementary material.

Acknowledgements

References

Alsop GB, Zhang D. Microtubules are the only structural constituent of the spindle apparatus required for induction of cell cleavage. J. Cell Biol 2003;162:383–390. [PubMed: 12900392]

Bakal CJ, Finan D, LaRose J, Wells CD, Gish G, Kulkarni S, DeSepulveda P, Wilde A, Rottapel R. The Rho GTP exchange factor Lfc promotes spindle assembly in early mitosis. Proc. Nat'l. Acad. Sci 2005;102:9529–9534.

Bement WM, Benink HA, von Dassow G. A microtubule-dependent zone of active RhoA during cleavage plane specification. J. Cell Biol 2005;170:91–101. [PubMed: 15998801]

Benink HA, Mandato CA, Bement WM. Analysis of cortical flow models in vivo. Mol. Biol. Cell 2000;11:2553–2563. [PubMed: 10930453]

Birkenfeld J, Nalbant P, Bohl BP, Pertz O, Hahn KM, Bokoch GM. GEF-H1 Modulates Localized RhoA Activation during Cytokinesis under the Control of Mitotic Kinases. Devel. Cell 2007;12:699–712. [PubMed: 17488622]

Bringmann H, Cowan CR, Kong J, Hyman AA. LET-99, GOA-1/GPA-16, and GPR-1/2 are required for aster-positioned cytokinesis. Curr. Biol 2007;17:185–191. [PubMed: 17189697]

Bringmann H, Hyman A. A cytokinesis furrow is positioned by two consecutive signals. Nature 2005;436:731–734. [PubMed: 16079852]

Canman JC, Cameron LA, Maddox PS, Straight A, Tirnauer JS, Mitchison TJ, Fang G, Kapoor TM, Salmon ED. Determining the position of the cell division plane. Nature 2003;424:1074–1078. [PubMed: 12904818]

Canman JC, Hoffman DB, Salmon ED. The role of pre- and post-anaphase microtubules in the cytokinesis phase of the cell cycle. Curr. Biol 2000;10:611–614. [PubMed: 10837228]

Cao L-H, Wang Y-L. Mechanism of the formation of the contractile ring in dividing cultured animal cells. II. Cortical movement of micro-injected actin filaments. J. Cell Biol 1990;111:1905–1911. [PubMed: 2229180]

Charras GT, Hu C-K, Coughlin M, Mitchison TJ. Reassembly of contractile actin cortex in cell blebs. J. Cell Biol 2006;175:477–490. [PubMed: 17088428]

D'Avino PP, Savoian MS, Capalbo L, Glover DM. RacGAP50C is sufficient to signal cleavage furrow formation during cytokinesis. J. Cell Sci 2006;119:4402–4408. [PubMed: 17032738]

DeBasio RL, LaRocca GM, Post PL, Taylor DL. Myosin II transport, organization, and phosphorylation: evidence for cortical flow/solation-contraction coupling during cytokinesis and cell locomotion. Mol. Biol. Cell 1996;7:1259–1282. [PubMed: 8856669]

Effler JC, Kee Y-S, Berk JM, Tran MN, Iglesias PA, Robinson DN. Mitosis-specific mechanosensing and contractile-protein redistribution control cell shape. Curr. Biol 2006;16:1962–1967. [PubMed: 17027494]

Fishkind DJ, Silverman JD, Wang Y-L. Function of spindle microtubules in directing cortical movement and actin filament organization in dividing cultured cells. J. Cell Sci 1996;109:2041–2051. [PubMed: 8856500]

Gerisch G, Bretschneider T, Muller-Taubenberger A, Simmeth E, Ecke M, Diez S, Anderson K. Mobile actin clusters and traveling waves in cells recovering from actin depolymerization. Biophysical J 2004;87:34993–3503.

Guha M, Zhou M, Wang Y-L. Cortical actin turnover during cytokinesis requires myosin II. Curr. Biol 2005;15:732–736. [PubMed: 15854905]

Janetopoulos C, Devreotes P. Phosphoinositide signaling plays a key role in cytokinesis. J. Cell Biol 2006;174:485–490. [PubMed: 16908667]

Jantsch-Plunger V, Gonczy P, Romano A, Schnabel H, Hamill D, Schnabel R, Hyman AA, Glotzer M. CYK-4: A Rho Family GTPase Activating Protein (GAP) Required for Central Spindle Formation and Cytokinesis. J. Cell Biol 2000;149:1391–1404. [PubMed: 10871280]

Kamijo K, Ohara N, Abe M, Uchimura T, Hosoya H, Lee J-S, Miki T. Dissecting the role of rho-mediated signaling in contractile ring formation. Mol. Biol. Cell 2006;17:43–55. [PubMed: 16236794]

Kanada M, Nagasaki A, Uyeda TQP. Adhesion-dependent and contractile ring-independent equatorial furrowing during cytokinesis in mammalian cells. Mol. Biol. Cell 2005;16:3865–3872. [PubMed: 15944220]

Kolega J. Phototoxicity and photoinactivation of blebbistatin in UV and visible light. BBRC 2004;320:1020–1025. [PubMed: 15240150]

Krendel M, Zenke FT, Bokoch GM. Nucleotide exchange factor GEF-H1 mediates cross-talk between microtubules and the actin cytoskeleton. Nat. Cell Biol 2002;4:294–301. [PubMed: 11912491]

Kurz T, Pintard L, Willis JH, Hamill DR, Gonczy P, Peter M, Bowerman B. Cytoskeletal regulation by the Nedd8 ubiquitin-like protein modification pathway. Science 2002;295:1294–1298. [PubMed: 11847342]

Mandato CA, Bement WM. Contraction and polymerization cooperate to assemble and close actomyosin rings around Xenopus oocyte wounds. J. Cell Biol 2001;154:785–797. [PubMed: 11502762]

Mishima M, Kaitna S, Glotzer M. Central spindle assembly and cytokinesis require a kinesin-like protein/ RhoGAP complex with microtubule bundling activity. Devel. Cell 2002;2:41–54. [PubMed: 11782313]

Motegi F, Sugimoto A. Sequential functioning of the ECT-2 RhoGEF, RHO-1 and CDC-42 establishes cell polarity in Caenorhabditis elegans embryos. Nat. Cell Biol 2006;8:978–985. [PubMed: 16921365]

Motegi F, Velarde NV, Piano F, Sugimoto A. Two phases of astral microtubule activity during cytokinesis in C. elegans embryos. Devel. Cell 2006;10:509–520. [PubMed: 16580995]

Munro E, Nance J, Priess JR. Cortical flows powered by asymmetrical contraction transport Par proteins to establish and maintain anterior-posterior polarity in the early C. elegans embryo. Devel. Cell 2004;7:413–424. [PubMed: 15363415]

Murthy K, Wadsworth P. Myosin-II-dependent localization and dynamics of F-actin during cytokinesis. Curr. Biol 2005;15:724–731. [PubMed: 15854904]

Nishimura Y, Yonemura S. Centralspindlin regulates ECT2 and RhoA accumulation at the equatorial cortex during cytokinesis. J. Cell Sci 2006;119:104–114. [PubMed: 16352658]

O'Connell CB, Warner AK, Wang Y-L. Distinct role of the equatorial and polar cortices in the cleavage of adjacent cells. Curr. Biol 2001;11:702–707. [PubMed: 11369234]

O'Connell CB, Wheatley SP, Ahmed S, Wang Y-L. The small GFP-binding protein Rho regulates cortical activities in cultured cells during division. J. Cell Biol 1999;144:305–313. [PubMed: 9922456]

Palazzo A, Cook TA, Alberts A,S, Gundersen GG. mDia mediates Rho-regulated formation and orientation of stable microtubules. Nat. Cell Biol 2001;3:723–730. [PubMed: 11483957]

Paluch E, van der Gucht J, Sykes C. Cracking up: symmetry breaking in cellular systems. J. Cell Biol 2006;175:687–692. [PubMed: 17145960]

Raich WB, Moran AN, Rothman JH, Hardin J. Cytokinesis and midzone microtubule organization in Caenorhabditis elegans require the kinesin-like protein Zen-4. Mol. Biol. Cell 1998;9:2037–2049. [PubMed: 9693365]

Rappaport, R. Cytokinesis in animal cells. Cambridge University Press; Cambridge, U.K.: 1996.

Rusan N, Tulu US, Fagerstrom C, Wadsworth P. Microtubule rearrangment in prophase/prometaphase cells requires cytoplasmic dynein. J. Cell Biol 2002;158:997–1003. [PubMed: 12235119]

Rusan NM, Fagerstrom C, Yvon AC, Wadsworth P. Cell cycle dependent changes in microtubule dynamics in living cells expressing GFP-alpha tubulin. Mol. Biol. Cell 2001;12:971–980. [PubMed: 11294900]

Sekine A, Fujiwara M, Narumiya S. Asparagine residue in the rho gene product is the modification site for botulinum ADP-ribosyltransferase. J. Biol. Chem 1989;91:8602–8605. [PubMed: 2498316]

Straight A, Cheung A, Limouze J, Chen I, Westwood NJ, Sellers JR, Mitchison TJ. Dissecting temporal and spatial control of cytokinesis with a myosin II inhibitor. Science 2003;299:1743–1747. [PubMed: 12637748]

Theriot JA, Mitchison TJ, Tilney LG, Portnoy DA. The rate of actin-based motility of intracellular Listeria monocytogenes equals the rate of actin polymerization. Nature 1992;357:257–260. [PubMed: 1589024]

Uehata M, Narumiya S. Calcium sensitization of smooth muscle mediated by a Rho-associated protein kinase in hypertension. Nature 1997;389:990–994. [PubMed: 9353125]

Wadsworth P. Cytokinesis: Rho marks the spot. Curr. Biol 2005;15:R871–874. [PubMed: 16271857]

Watanabe N, Madaule P, Reid T, Ishizaki T, Watanabe G, Kakizuka A, Saito Y, Nakao K, Jockusch BM, Narumiya S. p140mEia, a mammalian homolog of Drosophila diaphanous, is a target protein for Rho small GTPase and is a ligand for profilin. EMBO J 1997;16:3044–3056. [PubMed: 9214622]

Werner M, Munro E, Glotzer M. Astral signals spatially bias cortical myosin recruitment to break symmetry and promote cytokinesis. Curr. Biol 2007;17:1286–1297. [PubMed: 17669650]

Wheatley SP, Wang Y-L. Midzone microtubule bundles are continuously required for cytokinesis in cultured epithelial cells. J. Cell Biol 1996;135:981–989. [PubMed: 8922381]

White JG, Borisy GG. On the mechanism of cytokinesis in aimal cells. J. Theor. Bio 1983;101:289–316. [PubMed: 6683772]

Williams BC, Riedy MF, Williams EV, Gatti M, Goldberg ML. The Drosophila kinesin-like protein KLP3A is a midbody component required for central spindle assembly and initiation of cytokinesis. J. Cell Biol 1995;129:709–723. [PubMed: 7730406]

Wolpert L. The mechanics and mechanism of cleavage. Int. Rev. Cytol 1960;10:163–216.

Yoshizaki H, Ohba Y, Kurokawa K, Itoh R, Nakamura T, Mochizuki N, Nagashima K, Matsuda M. Activity of Rho-family GTPases during cell division as visualized with FRET-based probes. J. Cell Biol 2003;162:223–232. [PubMed: 12860967]

Yoshizaki H, Ohba Y, Parrini MC, Dulyaninova NG, Bresnick AR, Mochizuki N, Matsuda M. Cell type-specific regulation of RhoA activity during cytokinesis. J. Biol. Chem 2004;279:44756–44762. [PubMed: 15308673]

Yuce O, Piekny A, Glotzer M. An ECT2-centralspindlin complex regulates the localization and function of RhoA. J. Cell Biol 2005;170:571–582. [PubMed: 16103226]

Zhao W, Fang G. MgcRacGAP controls the assembly of the contractile ring and the initiation of cytokinesis. Proc. Natl. Acad. Sci. USA 2005;102:13158–13163. [PubMed: 16129829]

Zhou M, Wang YL. Distinct pathways for the early recruitment of myosin II and actin to the cytokinetic furrow. Mol. Bio. Cell 2008;19:318–326. [PubMed: 17959823]
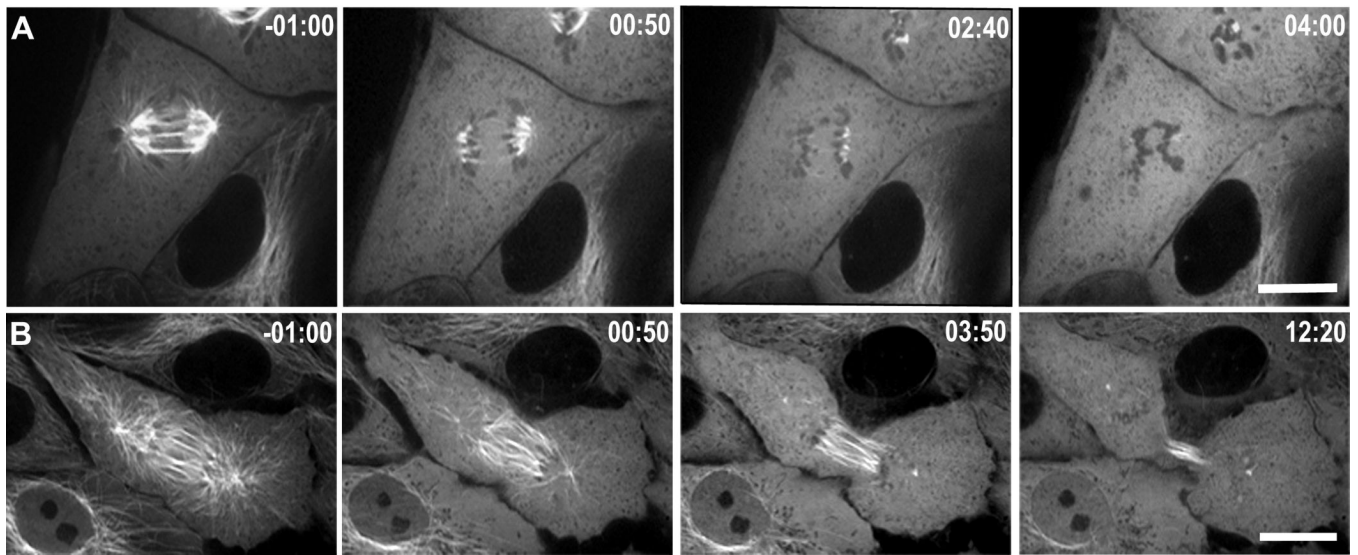
Figure 1. Differential stability of microtubules following anaphase onset
LLC-Pk1 cells stably expressing GFP-tubulin are shown before and at various times after the addition of 33μM nocodozole. (A) Addition of nocodazole within 2 minutes of anaphase onset induces rapid disassembly of microtubules and prevents cytokinesis; (B) addition of nocodazole > 2 minutes after anaphase onset results in disassembly of the majority of astral microtubules in the polar region and most astral microtubules in the equatorial region, but not interzonal, microtubules. Time in minutes:seconds relative to the addition of nocodazole Bars = 10 μm
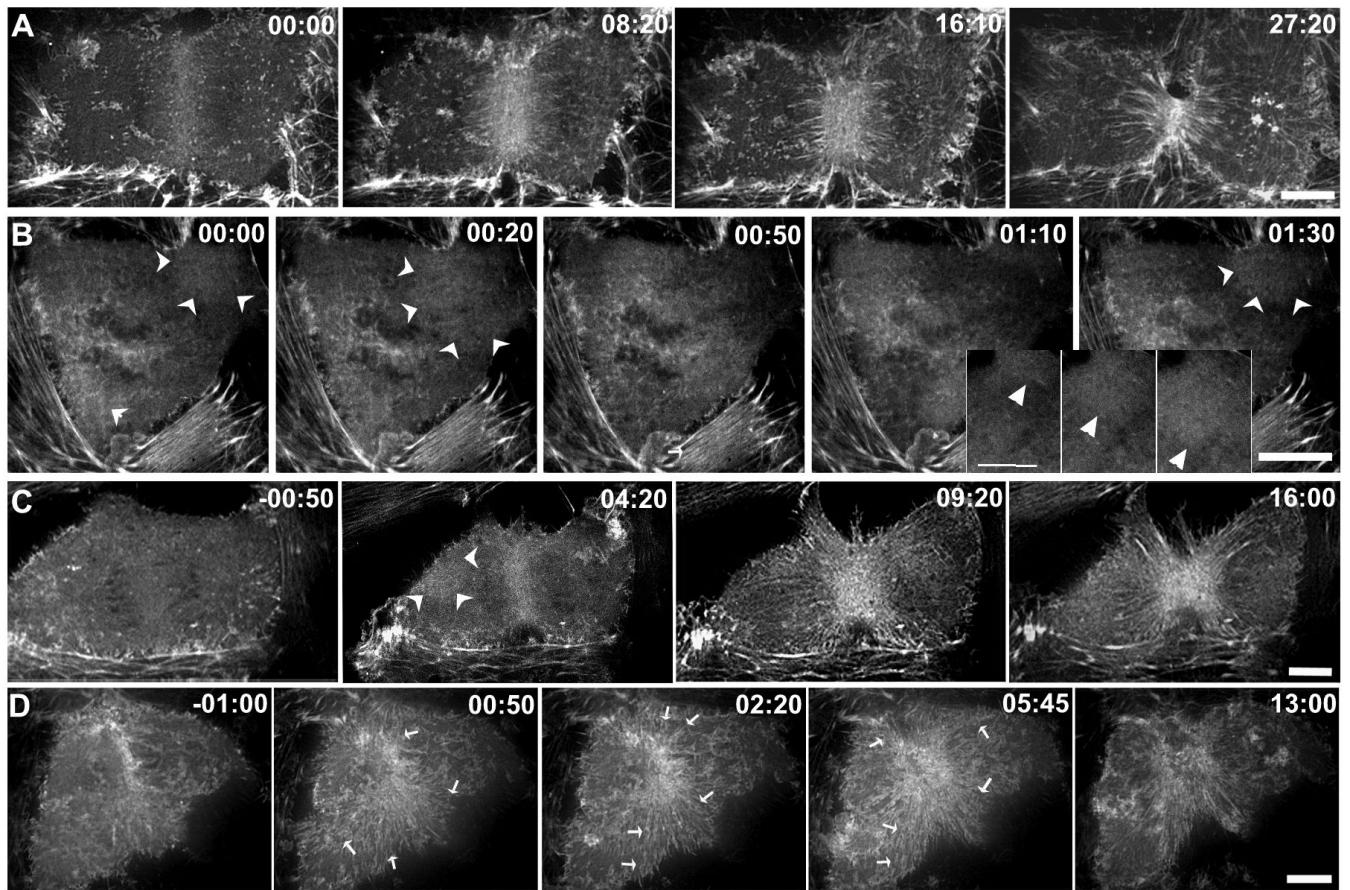
Figure 2. Microtubule disassembly induces changes in the organization of cortical actin
LLC-Pk1 cells stably expressing GFP-actin are shown before and at various times after addition of 33μM nocodozole. Contractile ring formation and cytokinesis in a control cell (A) and cells to which nocodazole was added either within 2 minutes (B) or > 2 minutes after (C, D) anaphase onset. In (B) both contractile ring assembly and cytokinesis fail, whereas in (C, D) furrow formation and ingression proceed. Wave-like behavior of cortical actin is shown in the inset panels in (B). Arrowheads mark wave-like behavior in (C,D). In (D) actin from distal regions of the cortex flows towards the equatorial region and contributes to the contractile ring; arrows mark the direction and region contributing to flow. Time in minutes:seconds relative to the addition of nocodozole in (B,C,D). Bars = 10 μm.
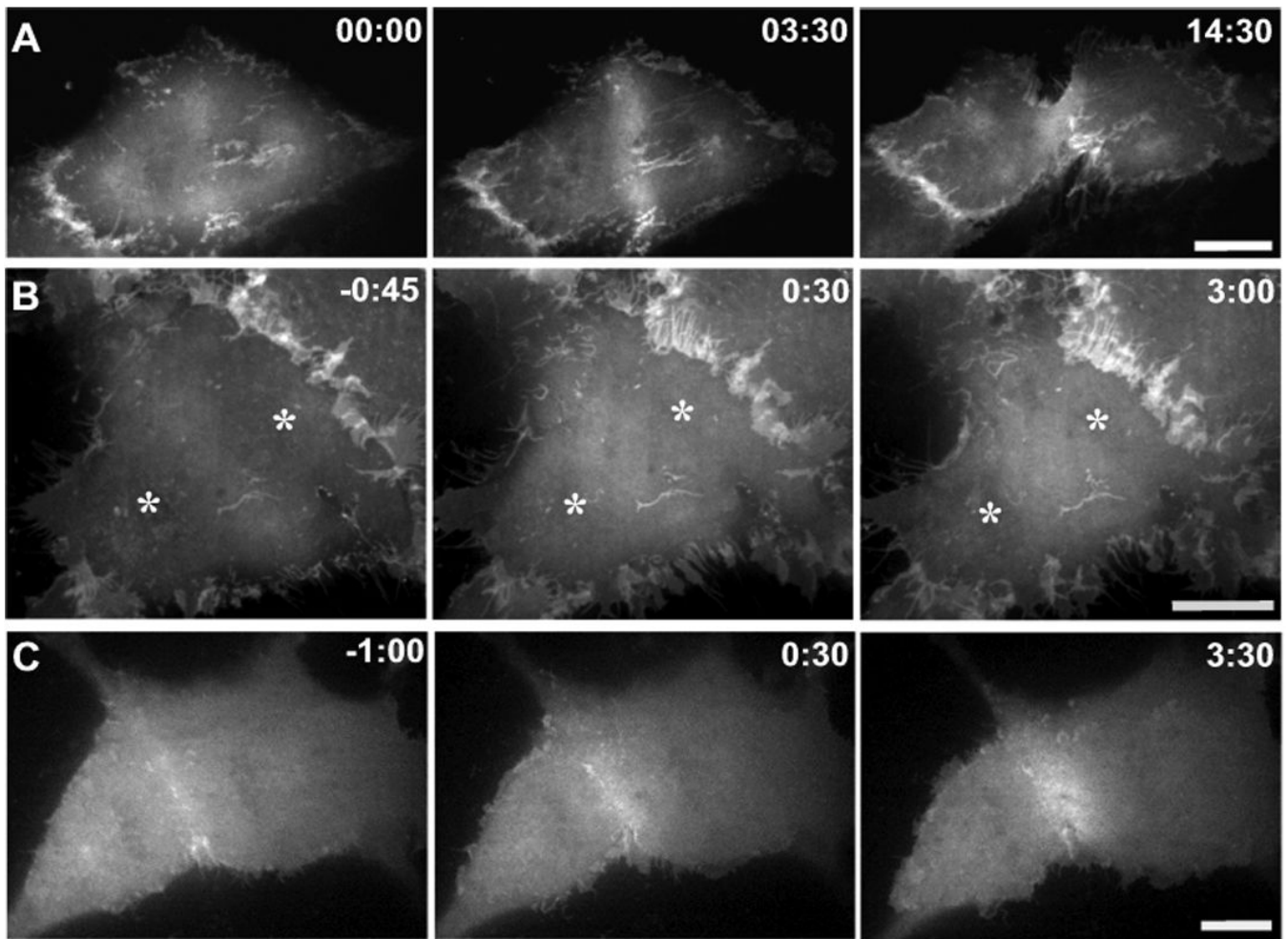
Figure 3. Localization of GFP-RhoA in control and in nocodazole treated cells
Fluorescence images of living LLC-Pk1 cells transfected with GFP-tagged *C.elegans* RhoA
(GFP-CeRhoA). In control cells (A) and nocodazole treated cells that assemble a contractile
ring (C), GFP-CeRhoA localizes to the equatorial cortex during cytokinesis. In nocodazole
treated cells that fail to assemble a contractile ring (B), GFP-CeRhoA fails to accumulate at
the equatorial region; asterisks mark the location of chromosomes. In both control and
nocodazole treated cells GFP-CeRhoA also localizes to membranous folds between
neighboring cells. Time is in min:sec. Bar = 10 μm.
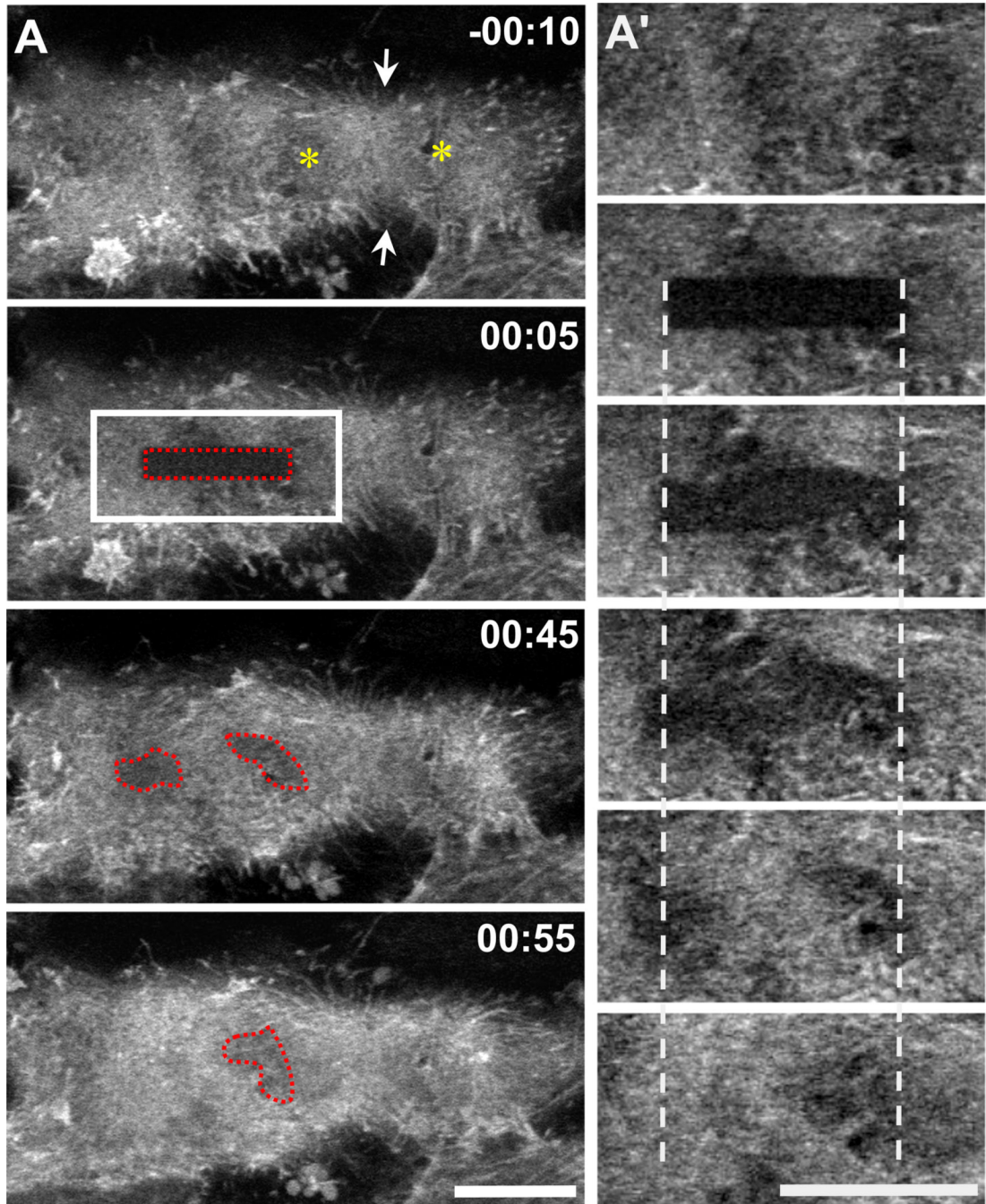
Figure 4. Actin polymerization and cortical contractions contribute to wave-like behavior of cortical actin in nocodazole treated anaphase cells

LLC-Pk1 cells expressing GFP-actin were followed until anaphase onset, nocodazole was added and photobleaching performed; red dotted region indicates the photobleached region; white boxes indicate the region that is shown in (A'); asterisks mark location of chromosomes; arrows mark site of cortical ingression. Time in min:sec relative to photobleaching. Bars = 10μm.
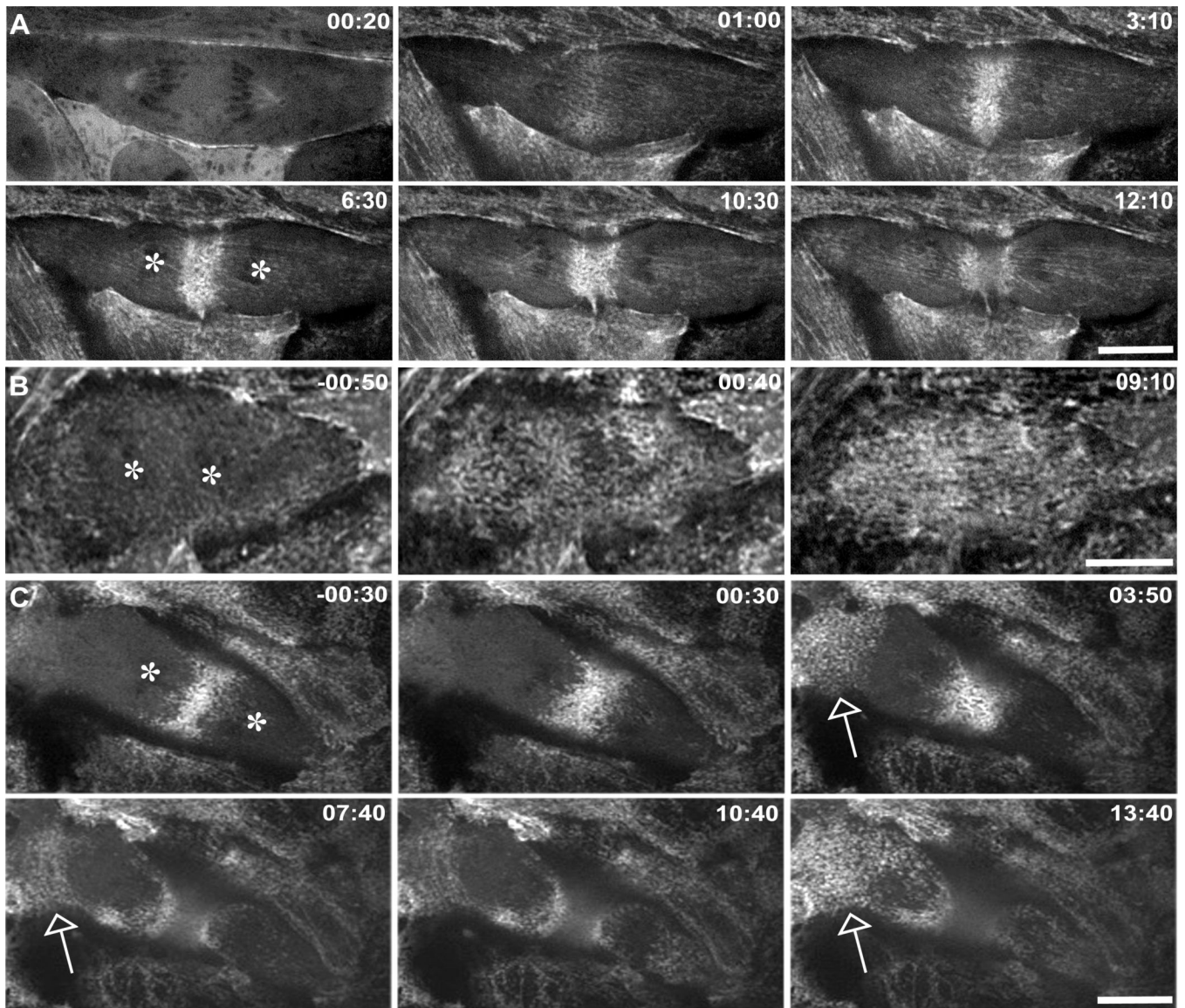
Figure 5. Mislocalization of TDRFP-Myosin RLC in nocodazole treated anaphase cells
(A-C) LLC-Pk1 cells stably expressing TDRFP-myosin regulatory light chain (MRLC). In control cells (A) TDRFP-MRLC accumulates at the equatorial cortex. (B) In nocodazole treated cells that fail to assemble a contractile ring, TDRFP-MRLC is diffusely distributed along the ventral cortex. (C) In nocodazole treated cells that assemble a contractile ring, myosin accumulates at the equatorial cortex, and shows transient accumulation in the polar cortex (arrows), compare 00:30 with 03:50. The first two frames are focused on the accumulation of MRLC at the equator, and as soon as contractile activity is observed away from the ring at 3:50, the focus shifts to the non-equatorial cortex. Time in upper right in minutes:seconds is relative to the addition of nocodazole. Asterisks mark the position of the chromosomes. Bars = 10μm.
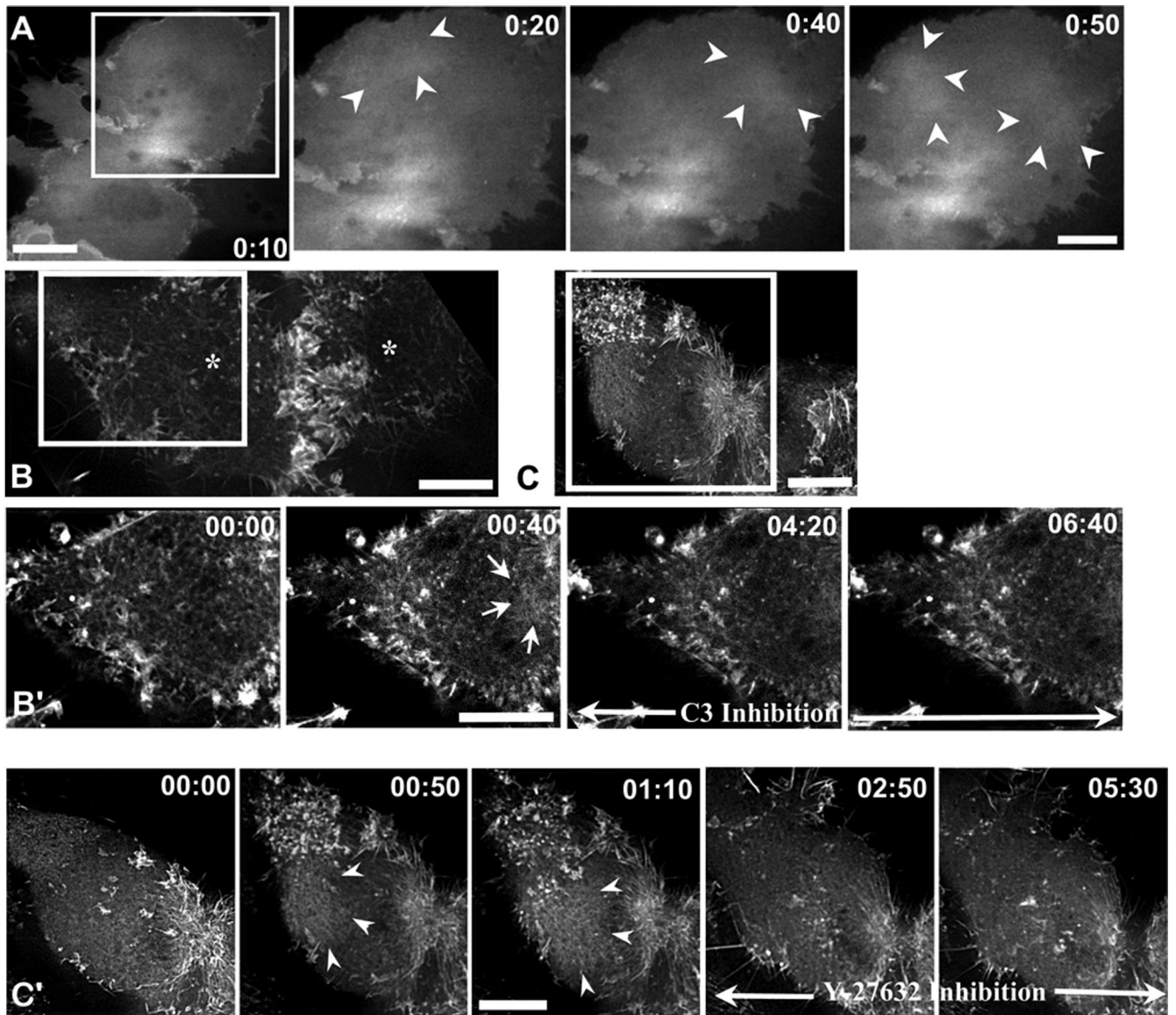
Figure 6. Rho is mislocalized and its activity is required for wave-like behavior of cortical actin in nocodazole treated cells
(A) GFP-CeRhoA is mislocalized to the polar region in nocodazole treated cells; arrowheads mark an area of GFP-CeRhoA fluorescence in the polar cortex. (B, C) LLC-Pk1 cells expressing GFP-actin were treated with nocodazole in anaphase, and then injected with C3 (B) or treated with Y-27632 (C). White boxes indicate the region that is shown in (B', C'). Addition of either C3 or Y-27632 suppresses wave-like behavior (B', C'); arrows show sites where cortical actin accumulated during wave-like behavior following treatment with nocodazole. Time of addition of C3 or Y27632 is indicated by black arrow. Time is in min:sec. Bars = 10 µm.
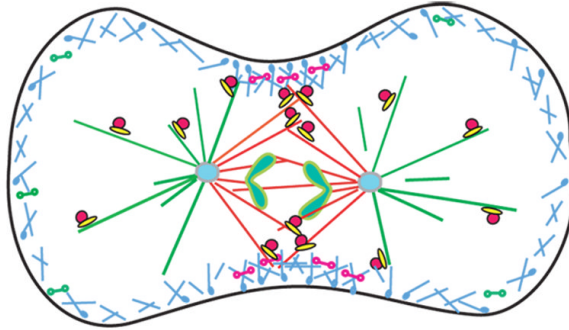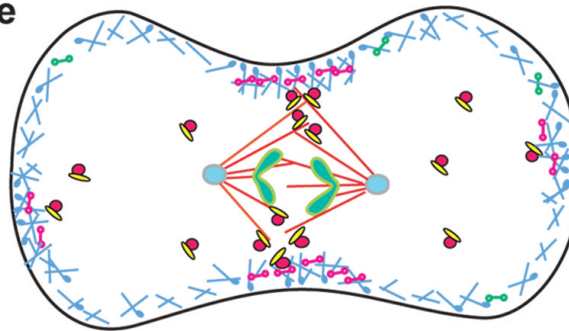
Figure 7. Model of microtubule dependent regulation of cortical actomyosin
Red lines, differentially stable and green lines dynamic microtubules; blue lines, F-actin;
yellow and red complexes, centralspindilin and RhoGEF. Dumbbells represent myosin II in
the inactive (green) and active form (pink). See text for details.

Table 1

Dynamics of actin in the contractile ring of control and nocodazole treated cells

	Percent recovery (%)	Half time recovery (s)
Control _n= 6_	68.0 ± 7.9[*]	29.8 ± 0.9
Nocodazole _n = 9_	50.3 ± 6.9	15.0 ± 1.0

[*] Values are Average ± Standard Deviation